Physica B 406 (2011) 693–698

Contents lists available at ScienceDirect

Physica B

journal homepage: www.elsevier.com/locate/physb

Evidence of formation of tetravacancies in uniformly oxygen irradiated n-type silicon

S.K. Chaudhuri [a,*], K. Goswami [b], S.S. Ghugre [a], D. Das [a]

[a] UGC-DAE Consortium for Scientific Research, Kolkata Centre, III/LB—8, Salt Lake, Kolkata-700098, India
[b] Department of Physics, Jadavpur University, 188 Raja S. C. Mallik Road, Kolkata-700032, India

ARTICLE INFO

Article history:
Received 19 July 2010
Received in revised form
26 October 2010
Accepted 1 December 2010

Keywords:
Positron annihilation spectroscopy
Silicon
Vacancy type defects
Radiation damage

ABSTRACT

High purity n-type silicon single crystal with resistivity in the order of 4000 Ω cm has been irradiated with high-energy oxygen ions at room temperature up to a fluence of 5E15 ions/cm^2. The energy of the beam was varied from 3 to 140 MeV using a rotating degrader to achieve a depthwise near-uniform implantation profile. Radiation induced defects and their dynamics have been studied using positron annihilation spectroscopy along with isochronal annealing up to 700 °C in steps of 50 °C for 30 min. After annealing the sample at 200 °C for 30 min, formation of silicon tetravacancies has been noticed. The formation of the tetravacancies was found to be due to agglomeration of divacancies present in the irradiated sample. An experimentally obtained positron lifetime value of 338 ± 10 ps has been reported for silicon tetravacancies, which has a very close agreement with the value obtained from recent theoretical calculations. The tetravacancies were found to dissociate into trivacancy clusters upon further annealing. The trivacancies thus obtained were observed to agglomerate beyond 400 °C to form larger defect clusters. Finally, all the defects were found to anneal out after annealing the sample at 650 °C.

1. Introduction

Radiation damage study in silicon crystal is important as radiation-induced defects substantially affect the behavior of the devices fabricated out of it. Nuclear radiation detectors, when placed in radiation environment, show gradual changes in their vital properties with time, like deterioration of resolution, increase in leakage current, etc., eventually prohibiting their long-term use as measurement devices [1–3]. Several types of radiation-induced defects have been identified till date in silicon. Defects like monovacancies (*V*), divacancies (V_2), vacancy–oxygen (*V–O*) complexes and vacancy phosphorus (*V—P*) complexes have been studied in great detail. Techniques like electron paramagnetic resonance [4], infrared spectroscopy [5], deep level transient spectroscopy [6] and positron annihilation spectroscopy (PAS) [7] have been heavily employed to identify and characterize these defects.

Theoretical calculations [8–10] do support the fact that formation of vacancy complexes like V_2, V_3, V_4, V_5, V_6, etc., is quite possible in silicon. But except in the case of V_2, very few experimental data are available in the existing literature regarding the nature of higher order vacancy complexes. Divacancies can be readily introduced into the silicon crystal using electron or other ion-irradiation; hence, have been studied in great detail [11,6]. Higher order vacancy complexes can be studied when there is a possibility of agglomeration of smaller vacancy clusters to form a higher order vacancy complex. The agglomeration process can take place during irradiation or during post irradiation treatment like thermal annealing when smaller vacancy clusters acquire sufficient mobility upon heat treatment [12]. But again, as pointed out by Haley et al. [13], vacancy clustering process on thermal treatment depends on several factors such as the cluster size, vacancy interaction range, vacancy concentration, etc., leading to uncertainty in the formation of a particular vacancy cluster.

The present article reports the formation of four-vacancy clusters, also known as tetravacancies that are denoted by V_4, during annealing of oxygen irradiated FZ grown n-type silicon crystal. Deliberate introduction of oxygen in silicon crystal is a very effective technique to fabricate radiation-hardened detectors [14]. High-energy oxygen ions can be used to get them implanted deep inside the crystal, which is needed for fabrication of a practical radiation-hardened detector, but the process of ion-implantation introduces several defects in the crystal. In order to remove these defects it is required to anneal the irradiated sample prior to detector fabrication. The thermal annealing in the present case has been carried out in intervals of 50 °C and the radiation induced defects have been studied at each step. Each annealing step was of 30 min duration. This type of measurement facilitates the study of defect dynamics and determination of actual temperature of a particular type of defect to anneal out. The defects have been characterized using positron annihilation lifetime spectroscopy (PALS) and Doppler broadening of positron annihilation radiation

* Corresponding author.
E-mail address: s.chaudhuri@surrey.ac.uk (S.K. Chaudhuri).

0921-4526/$ - see front matter © 2010 Elsevier B.V. All rights reserved.
doi:10.1016/j.physb.2010.12.001

(DBPAR) spectroscopy. Positron annihilation spectroscopy is a very effective tool to detect and identify vacancy type defects and their complexes in semiconductors [7].

In the present article, we report the experimentally obtained positron lifetime in silicon tetravacancy. The experimentally obtained value has been found to be in very good agreement with the results of most recent theoretical calculations. The formation mechanism and stability of the tetravacancies have been discussed and were compared with existing reports in the literature on tetravacancies in silicon. From the available theoretical calculations, the structure of the tetravacancies detected in the present study is proposed to be of "part-of-a-hexagonal-ring" (PHR) configuration.

2. Experimental details

N-type detector-grade silicon wafer (resistivity $\sim$4000 Ω cm) of thickness around 500 μm and diameter about 15 mm were sliced from an ingot along the ⟨1 1 1⟩ crystal plane. The crystal was irradiated with 140 MeV oxygen ions (O^{6+}) up to a fluence of 5×10^{15} ions/cm^2 using the beam-line of Variable Energy Cyclotron Centre (VECC), Kolkata, India. The energy of the beam from the cyclotron was varied using a rotating degrader. The rotating degrader is a rotating mechanical wheel containing slots fitted with aluminium absorbers of different thicknesses placed in the path of the beam. As a result, the energy of the outgoing beam from the degrader varied in a regular cyclic manner from 140 to 3 MeV. The details of the experimental set up can be found in Ref. [15]. The outgoing beam energies and their corresponding ranges in the sample have been illustrated in Fig. 1.

For PALS and DBPAR measurements a 12 μCi ^{22}Na positron source (deposited on aluminium foil) has been used. The PALS system used in this work was a standard fast–fast coincidence setup with two identical 1 in. tapered-off BaF_2 scintillator detectors fitted with XP2020Q photomultiplier tubes. The time resolution obtained using ^{60}Co source with ^{22}Na gates was 290 ps. A total of more than 1 million counts were recorded for each lifetime spectrum. All lifetime spectra were analyzed using PATFIT 88 program [16] after background and source corrections. A total of 15% contribution from the source and an average background count of 20 per channel have been incorporated as corrections during the analysis. The source correction was carried out following the procedure adopted by Staab et al. [17]. Up to an annealing temperature of 600 °C, all lifetime spectra of the irradiated samples were deconvoluted using one Gaussian resolution function with two exponential lifetimes. Beyond 600 °C, a single component fit gave satisfactory results. DBAR spectra were recorded for two hours using a single HPGe detector with an energy resolution of 1.7 keV for 662 keV gamma rays from a ^{137}Cs standard source. Doppler broadened energy spectra were analyzed using the code SP (version 1.0) [18] to calculate the *S*-parameter. The *S*-parameter has been calculated as the ratio of number of counts integrated under a central segment spreading over $\pm$0.8 keV around the centroid of the 511 keV annihilation peak to the number of counts under the full spectrum.

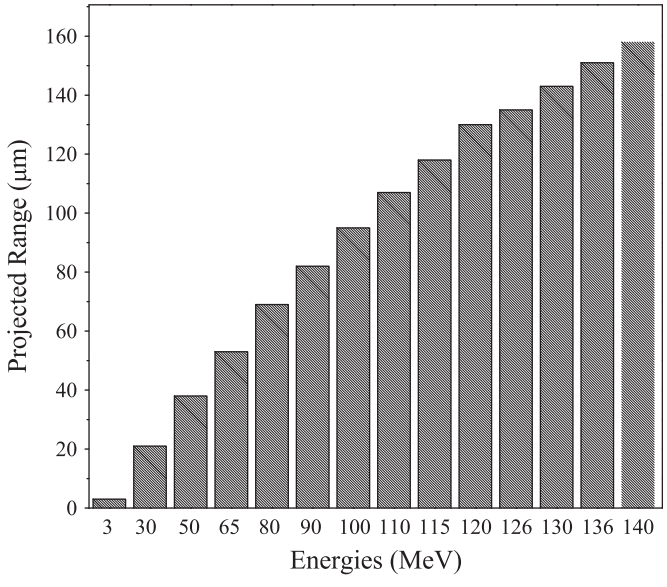

Fig. 1. Beam energies obtained from the rotating degrader and their corresponding ranges in silicon.

The isochronal annealing treatments were carried out in the temperature range 100–700 °C in intervals of 50 °C. Each annealing was carried out in vacuum ($\sim10^{-5}$ mbar) for 30 min. Several data (PALS as well as DBPAR) were retaken and reanalyzed and the resolution and peak position were monitored intermittently to check the reproducibility of the results and the stability of the spectrometer. A reasonably good reproducibility and stability of the spectrometer was observed over the entire period of experiment. During the deconvolution process the variance of a fit was minimized to obtain the best fit and at the same time the standard deviations of the individual lifetime parameters were checked not to give abnormally large values even if it shows a lesser variance in the overall fit.

3. Results and discussion

3.1. Doppler broadening of annihilation radiation studies

The Doppler broadening of the 511 keV annihilation gamma peak reflects momentum distribution of the annihilating electrons. In open volume defects, because of significantly low momentum of the valence electrons, the momentum distribution of annihilating electrons shifts to smaller values; hence, Doppler broadening of the annihilation line decreases [19]. Therefore, the annihilation peak of a defect-rich sample becomes higher and narrower compared with that of a defect-free sample, when both the peaks are normalized to equal area. As a result of this, *S*-parameter of a defect-rich sample becomes higher compared with that of a defect-free sample. However, the value of *S*-parameter so obtained, is the weighted average of *S*-parameters for positrons annihilating in the defect-free bulk region (S_b) as well as those trapped in the vacancy type defects (S_d). S_d can be calculated using the relations

$$S=(1-f)S_b+f\,S_d \tag{1}$$

where

$$f=K/(K+\tau_b^{-1}) \tag{2}$$

and K is the trapping rate of positrons in the vacancy type defects obtained from lifetime measurements (will be discussed in details in the next section) and τ_b is positron lifetime in bulk.

Fig. 2 shows the variation in S_d of the irradiated sample as a function of annealing temperature. It increases sharply at 200 °C, then falls to lower value and then maintains a more or less constant value up to 400 °C and again increases gradually up to an annealing temperature of 500 °C. Since *S*-parameter is sensitive to both concentration and size of the defects, the observed increase in the defect related *S*-parameter values may be due to vacancy agglomeration or may be due to increase in concentration of a particular type of defect as well. A confirmatory answer can be obtained by studying the deconvoluted lifetime parameters (to be discussed in the next section). Beyond 500 °C, the defect related

S-parameter gradually decreases. At 700 °C the *S*-parameter reaches a value (Table 1) almost equal to that obtained for the defect-free sample, indicating complete annealing out of vacancies.

3.2. Positron annihilation lifetime studies

Lifetime of a positron inside a material depends on its average electron density. Lifetime of a positron increases when it is trapped in a vacancy type defect because of the low local electron density at the defect site. From the defect related lifetime, extracted from the positron annihilation lifetime spectrum, the size of the defect can be easily determined and its relative concentration can be determined from the corresponding intensity. All the lifetime spectra of the irradiated sample were deconvoluted using two lifetime components τ_1 and τ_2 with corresponding intensities I_1 and I_2, respectively. The shorter lifetime (τ_1) was attributed to the reduced bulk lifetime of positrons in silicon and the longer (τ_2) was ascribed to the lifetime of positrons trapped in vacancy type defects.

Fig. 3 shows the variation in positron mean lifetime as a function of annealing temperature. The mean lifetime was calculated from the deconvoluted positron lifetime parameters using the expression:

$$\tau_m = \frac{\tau_1 I_1 + \tau_2 I_2}{I_1 + I_2} \tag{3}$$

The mean lifetime thus obtained is not sensitive to the uncertainties involved in the numerical fitting and it can readily indicate the presence of vacancy type defects in a crystal. For comparison, the variation in positron lifetime of an n-type reference sample has also been plotted. The lifetime value obtained for the unirradiated sample is 218 ps, which is close to the positron lifetime in defect-free bulk silicon [20]. This indicates that the reference sample is free of vacancy type defects or their concentration is at least below the detection limit of positron lifetime spectroscopy. The positron lifetime in the reference sample was almost same throughout the annealing process. The positron mean lifetime for the as-irradiated sample obtained at room temperature and up to an annealing temperature of 550 °C is well above than that of bulk silicon, indicating the presence of vacancy type defects. Beyond 550 °C the mean lifetime begins decreasing, indicating the annealing of the vacancy type defects. Finally, at 650 and 700 °C, it was found that a two-component deconvolution of the lifetime spectrum of the irradiated sample was not possible and the best fit was obtained using a single component fit. This indicates complete annealing out of vacancy type defects from the irradiated sample at 650 °C, as has already been concluded from the *S*-parameter results.

In the case of presence of multiple types of defects in the sample with very close lifetime values, the numerical fitting programs may not deconvolute the lifetime spectra properly. This often leads to lifetime parameters that are admixture of two or more closely valued lifetimes. Trapping model analyses may help in investigating this types of cases. So, further analysis of the lifetime data was carried out with a two-state trapping model [21,22]. In this model, one bulk state and one trapped state with no de-trapping are assumed as probable sites for positron annihilation. As per the trapping model, the experimental lifetime τ_i and the intensities I_i ($i=1, 2$) are related to the characteristic lifetimes τ_b and τ_d by

$$\tau_1^{-1} = \tau_b^{-1} + K \tag{4}$$

$$I_2 = 1 - I_1 = \frac{K}{K + \tau_b^{-1} - \tau_d^{-1}} \tag{5}$$

where τ_b is the bulk lifetime, $\tau_d = \tau_2$ is the defect related lifetime and K is the trapping rate.

The trapping rate was calculated using Eq. (5) with the experimentally obtained value of τ_2 and I_2, and the reduced bulk lifetime τ_1^{TM} was calculated using Eq. (4) thereafter. A comparison

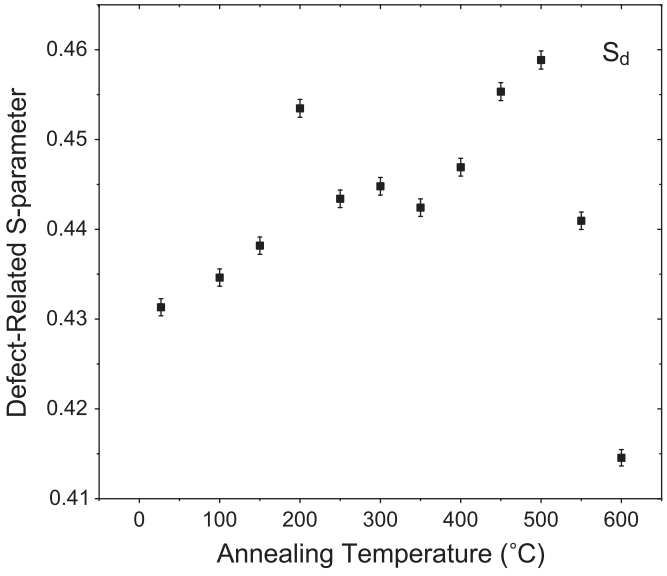

Fig. 2. Variation in defect related *S*-parameter (S_d) as a function of annealing temperature.

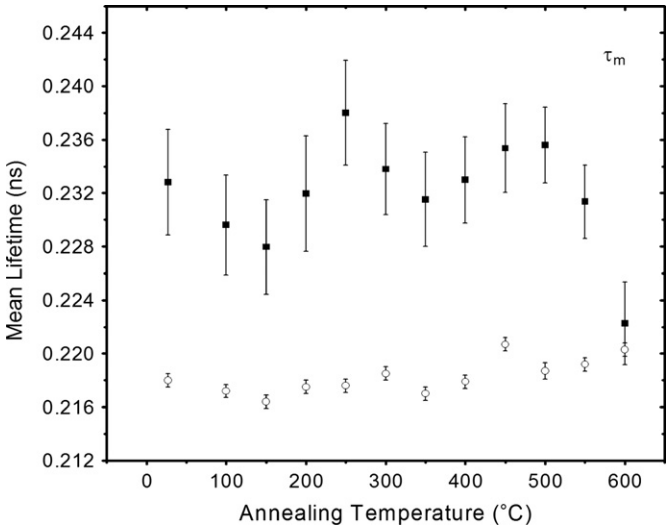

Fig. 3. Variation in positron mean lifetime as a function of annealing temperature for the irradiated sample (■). The open circles (○) represent the positron lifetime measured for the reference sample after each annealing step.

Table 1
Positron annihilation parameters of the unirradiated, irradiated and annealed sample.

Sample	τ_1 (ps)	τ_2 (ps)	I_1 (%)	I_2 (%)	*S*
Unirradiated	218 ± 1	–	–	–	0.40873 ± 0.00088
As-irradiated	178 ± 7	316 ± 8	60 ± 5	40 ± 5	0.41254 ± 0.00089
After annealing at 700 °C	219 ± 1	–	–	–	0.40978 ± 0.00090

of the lifetime τ_1^{TM}, calculated from the two-state trapping model, with the experimentally obtained lifetime τ_1 is performed to test whether the two-state trapping model is valid for the defects in the oxygen irradiated n-type silicon. The value of τ_b is taken as 218 ps. Fig. 4 shows the variations in τ_1 and τ_1^{TM} as functions of annealing temperature. It is evident from the figure that up to 450 °C the value of τ_1^{TM} is in good agreement with the experimental results. This indicates that the smallest lifetime τ_1 is a pure lifetime component, i.e., there are no such defects present in the sample, which has a lifetime close to the bulk lifetime. However, close values of τ_1 and τ_1^{TM} may not indicate that the lifetime component τ_2 is well resolved. In case the deconvoluted lifetime τ_2 is an admixture of positron lifetimes in two different kinds of defects, a two-state trapping model will be still valid as the situation may be assumed to be similar to positrons annihilating in bulk and a single defect site with a lifetime τ_2 rather than in two different defect sites. Moreover, a three-state trapping model, which assumes the presence of two different types of defects (having close lifetime values) and a bulk state in the sample, leads to an expression of trapping rate exactly similar to that of a two-state trapping model [23]. From this three-state trapping model, only the total trapping rate can be calculated and not the individual trapping rates in each defect. Hence, unlike in the case of two-state trapping model, the three-state trapping model cannot be used to test whether τ_2 is a purely resolved lifetime parameter or not.

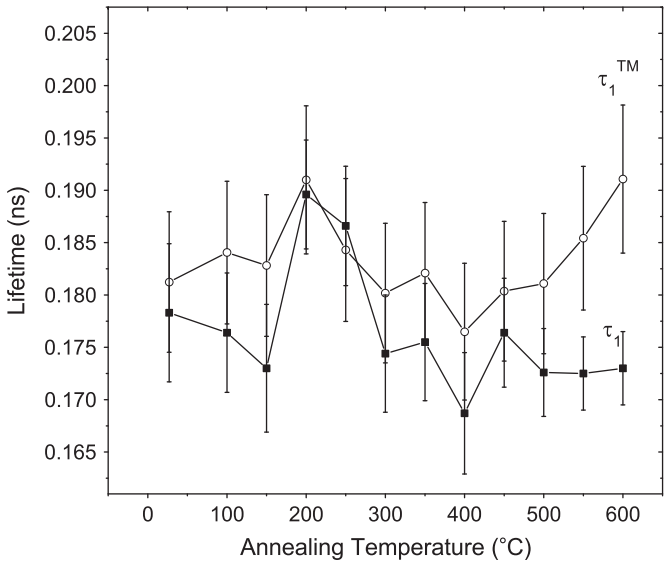

Fig. 4. Comparison of τ_1 values as obtained from experiment (■) with those calculated from two-state trapping model (○) (the lines joining the points are guide to eye).

A clearer picture of the defect dynamics can be obtained from the variation in the deconvoluted lifetime parameters with annealing temperature. Table 1 shows the values of the lifetime parameters of the reference and the as-irradiated samples. The defect related lifetime τ_2 of the as-irradiated sample shows a value of 315 ± 8 ps, indicating the presence of divacancies in the irradiated sample. An experimentally obtained lifetime value of divacancy, as reported by Polity et al. [24], is 310 ± 5 ps. Fig. 5 shows the behavior of defect related lifetime τ_2 and the corresponding intensity I_2 with change in annealing temperature. Up to 200 °C, τ_2 shows a slight increase and the corresponding intensity I_2 decreases. This is a clear indication of agglomeration of the divacancies. The value of τ_2 at 200 °C is 338 ± 10 ps. This value is close to that of theoretically calculated values of positron lifetime in tetravacancies in silicon. Theoretical calculations available in literature assume several models for lifetime calculations. For instance, the widely used nonself-consisitent (NSC) method [25,26] neglects the impact of the trapped positron in defects on the nearby electrons whereas more recent and accurate calculations like fully self-consistent method based on density functional theory (DFT) [27,28] optimizes the electron and positron densities self-consistently by taking into account these relaxation effects. However, DFT calculations of positron lifetime in multivacancies comprising three or more vacancies by Saito and Oshiyama [29] showed that relaxation effects are negligible for these defects. The experimentally obtained lifetime value at 200 °C, in the present case, has a close match with that calculated using the DFT and NSC method (334 and 340 ps, respectively) for tetravacancies in "part-of-a-hexagonal-ring" (PHR) [28]. Fujinami et al. [30] have also reported experimentally obtained lifetime value of tetravacancies between 343 and 330 ps.

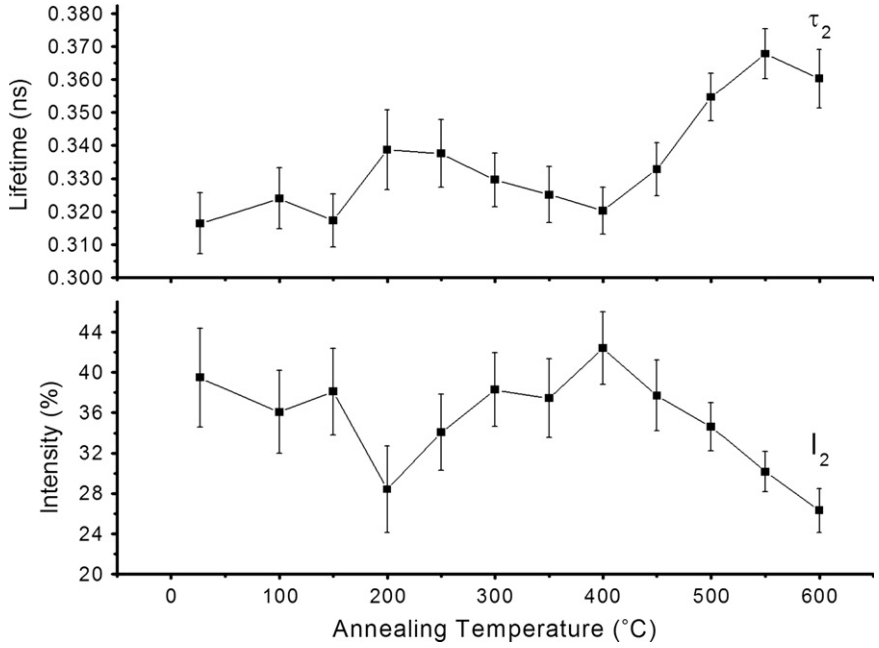

Fig. 5. Variation in defect related positron lifetime (τ_2) and intensity (I_2) as a function of annealing temperature (the lines joining the points are guide to eye).

The formation mechanism of the tetravacancies can be explained in a following manner. The divacancies might have become mobile at 200 °C and agglomerated to form four-vacancy clusters, which are energetically more stable than divacancies, following the reaction $V_2+V_2 \rightarrow V_4$ [31]. So, the defect related lifetime value of 338 ps at 200 °C is assigned to positrons annihilating in the tetravacancies. Above 250 °C, τ_2 is seen to decrease along with a increase in I_2. This is most probably a signature of dissociation of V_4 clusters. Theoretically it has been shown [32] that tetravacancies can dissociate via two channels with the following energetics. The reaction $V_4 \rightarrow V_3+V$ has a dissociation energy 1.92 eV and $V_4 \rightarrow V_2+V_2$ has a dissociation energy 2.31 eV, where V_3 stands for trivacancies and V for monovacancies. Between the two channels, the former channel seems to be more logical in this case for the following reasons. Apart from having lower formation energy, the theoretically calculated stability of trivacancies against dissociation is comparable to that of tetravacancies [32]. So, the existence of trivacancies at such high temperature seems to be feasible. Moreover, the monovacancies produced as a result of dissociation of the tetravacancies may also agglomerate to form trivacancies thereby further increasing the number of trivacancies. The corresponding increase in I_2 also supports this conclusion.

An interesting point to be noted here is that although the dissociation of tetravacancies into trivacancies began after annealing the sample at 250 °C, the process was not complete until the sample was annealed to 400 °C. This was inferred from the fact that the lifetime value τ_2 decreased slowly in this region. Had the dissociation process been drastic, lifetime value τ_2 should have decreased from that of tetra to trivacancies sharply, rather than acquiring values in between that of tetra and trivacancies. This is possible only when an experimentally obtained lifetime value is an admixture of two lifetimes, which are difficult to resolve otherwise. The region 250–400 °C in Fig. 5 thus indicates that the lifetime τ_2 is weighted average of positron lifetimes in tetra as well as in trivacancies. A gradual decrease in the fraction of tetravacancies has led to a gradual decrease in the lifetime value. At 400 °C the value of τ_2 is 320 ± 7 ps, which is also close to calculated positron lifetime in trivacancies (322 ps) [28], indicating the presence of trivacancies only.

It may be mentioned here that reports on the evidence of formation of tetravacancies using positron annihilation technique is meager in literatures. Dannefaer et al. [33], in one of their recent works, reported on the formation of tetravacancies in electron- and proton-irradiated FZ silicon following a similar mechanism as mentioned above. Also, in one of their earlier works, Dannefaer et al. [34] reported the formation of V_4 in neutron irradiated high purity and oxygen-lean p-type silicon when the sample was annealed at a temperature of 150 °C. Apart from these, Meng [35] reported a similar formation of V_4 following a similar mechanism in the temperature range 400–600 °C in neutron-transmutation-doped silicon irradiated with reactor neutrons, Fujinami et al. [30] reported formation of V_4 after annealing low-energy and low-dose oxygen-implanted CZ silicon at 600 °C, and Harding et al. [36] reported formation of vacancy clusters consisting of 3–4 silicon vacancies after annealing 4 MeV self-implanted silicon at 525 °C. The above-mentioned differences in the existing reports regarding the formation of V_4 might have occurred because the experimental conditions in all the cases were widely different such as different types of particles with different energies, fluence, etc. have been used. Moreover the initial oxygen concentration in the silicon material was different in different cases. These differences may render the damage structure of the irradiated portion different in different cases, and it is a well-known fact that the charge state of a vacancy complex in heavily damaged/quasi-amorphous regions can be different from that in a lesser-damaged area [37]. The charge state in turn controls the mobility of these defects, which further affects their agglomeration behavior [38]. Also the atomic structure (e.g. hexagonal, chain, four-fold symmetry, etc.) of multi-vacancy defects may play an important role in deciding their annealing temperature as has been reported by Lee and Corbett [39].

From 450 to 550 °C, another sign of agglomeration of the vacancy clusters, as manifested by the increase in τ_2 and decrease in I_2, can be seen. This has occurred most probably due to the gained mobility of the V_3 clusters at such high temperatures. It is also clear from Fig. 4 that a two-state trapping model is seen to be no longer valid beyond 450 °C, indicating the formation of defects having positron lifetime close to the bulk value. These defects may include vacancy–oxygen complexes. Formation of vacancy–oxygen complexes is highly probable in this case because the presence of oxygen in the sample in sufficient quantity. The departure from the trapping model is persistent beyond 550 °C also, indicating the presence of multiple types of defects in the sample for rest of the annealing temperatures. The gradual decrease in I_2 beyond 500 °C is a signature of annealing out of all these defects, and a single component fit at 650 and 700 °C indicates complete annealing out of all defects present in the crystal.

4. Conclusions

Radiation defects due to high-energy oxygen ion-bombardment in detector grade silicon have been studied using positron annihilation spectroscopy along with isochronal annealing. A rotating degrader has been used for near-uniform implantation of the oxygen atoms. Positron lifetimes obtained for the as-irradiated sample indicated formation of divacancies as a result of irradiation. These divacancies have been argued to agglomerate at 200 °C to form tetravacancies. A positron lifetime of 338 ± 10 ps has been reported for the tetravacancies which is also very close to recent theoretically calculated lifetime values. These tetravacancies have been found to dissociate into trivacancies. It appeared that the dissociation process did not complete till the sample was annealed at 400 °C. A further agglomeration of these trivacancies along with the possible formation of vacancy–oxygen complexes has also been reported. The defects were seen to disappear after annealing of the sample at 650 °C.

References

[1] V.A.J. Van Lint, Nucl. Instrum. Methods A 253 (1987) 453.
[2] G. Lutz, Nucl. Instrum. Methods A 377 (1996) 243.
[3] J. Kemmer, et al., Nucl. Instrum. Methods A 439 (2000) 19.
[4] G.D. Watkins, J.W. Corbett, Phys. Rev. 138 (1965) 543.
[5] L.J. Cheng, J.C. Correlli, J.W. Corbett, G.D. Watkins, Phys. Rev. 152 (1996) 761.
[6] B.G. Svensson, B. Mohadjeri, A. Hallén, J.H. Svensson, J.W. Corbett, Phys. Rev. B 43 (1991) 2292.
[7] R. Krause-Rehberg, H.S. Leipner, Positron Annihilation in Semiconductors, vol. 127, Springer, Berlin, 1999.
[8] N. Cuendet, T. Halicioglu, W.A. Tiller, Appl. Phys. Lett. 67 (1995) 1063.
[9] T.E.M. Staab, A. Sieck, M. Haugk, M.J. Puska, Th. Frauenheim, H.S. Leipner, Phys. Rev. B 65 (2002) 115210.
[10] D.V. Makhov, Laurent J. Lewis, Phys. Rev. Lett. 92 (2004) 255504.
[11] J.W. Corbett, G.D. Watkins, Phys. Rev. Lett. 7 (1961) 314.
[12] R. Poirier, V. Avalos, S. Dannefaer, F. Schiettekatte, S. Rooda, Physica B 340–342 (2003) 609.
[13] Benjamin P. Haley, M. Keith, Phys. Rev. B 74 (2006) 045217.
[14] G. Lindström, et al., Nucl. Instrum. Methods A 465 (2001) 60.
[15] S.K. Chaudhuri, K. Goswami, S.S. Ghugre, D. Das, J. Phys. Condens. Matter 19 (2007) 216206.
[16] P. Kirkegaard, M. Eldrup, Comput. Phys. Commun. 3 (1972) 240.
[17] T.E.M. Staab, B. Somieski, R. Krause-Rehberg, Nucl. Instrum. Methods A 381 (1996) 14.
[18] 〈http://positronannihilation.net/software.html〉.
[19] S. Szpala, P. Asoka-Kumar, B. Nielsen, J.P. Peng, S. Hayakawa, K.G. Lynn, H.-J. Gossmann, Phys. Rev. B 54 (1996) 4722.
[20] S. Dannefaer, Phys. Status Solidi A 102 (1987) 481.
[21] A. Seeger, J. Phys. F: Met. Phys. 3 (1973) 248.

[22] A. Vehanen, P. Hautojarvi, J. Johansson, J. Yli-Kauppila, Phys. Rev. B 25 (1982) 762.
[23] W. Brandt, in: A.T. Stewardt, L.O. Roellig (Eds.), Positron Annihilation, Academic Press, New York, 1967, p. 155.
[24] A. Polity, F. Börner, S. Huth, S. Eichler, R. Krause-Rehberg, Phys. Rev. B 58 (1998) 10363.
[25] M.J. Puska, R.M. Nieminen, J. Phys. F: Met. Phys. 13 (1983) 333.
[26] M.J. Puska, Phys. Status Solidi A 102 (1987) 11.
[27] I. Makkonen, M.J. Puska, Phys. Rev. B 76 (2007) 054119.
[28] D.V. Makhov, Laurent J. Lewis, Phys. Rev. B 71 (2005) 205215.
[29] M. Saito, A. Oshiyama, Phys. Rev. B 53 (1996) 7810.
[30] M. Fujinami, T. Miyagoe, T. Sawada, R. Suzuki, T. Ohdaira, T. Akahane, J. Appl. Phys. 95 (2004) 3404.
[31] T.E.M. Staab, M. Haugk, A. Sieck, Th. Frauenheim, H.S. Leipner, Physica B 273–274 (1999) 50.
[32] J.L. Hastings, S.K. Estreicher, P.A. Fedders, Phys. Rev. B 56 (1997) 10215.
[33] S. Dannefaer, V. Avalos, D. Kerr, R. Poirier, V. Shmarovoz, S.H. Zhang, Phys. Rev. B 73 (2006) 115202.
[34] S. Dannefaer, G.W. Dean, D.P. Kerr, B.G. Hogg, Phys. Rev. B 14 (1976) 2709.
[35] Xiang-Ti Meng, Phys. Scr. 50 (1994) 419.
[36] R. Harding, G. Davies, J. Tan, P.G. Coleman, C.P. Burrows, J. Wong-Leung, J. Appl. Phys. 100 (2006) 073501.
[37] H.H. Sander, B.L. Gregory, IEEE Trans. Nucl. Sci. 13 (1966) 53.
[38] L.C. Kimerling, H.M. DeAngelis, J.W. Diebold, Solid State Commun. 21 (1978) 1391.
[39] Young-Hoon Lee, James W. Corbett, Phys. Rev. B 9 (1974) 4351.